Photothermally Induced Alkyl Radicals and Pyroptosis Synergistically Inhibit Breast Tumor Growth

Yang Du[1,2], Lili Niu[1,2,3], Nannan Li[1,2,3], Huishu Guo[1,2] *

1. Central Laboratory, First Affiliated Hospital, Dalian Medical University, Dalian 116021, China.

2. The Institute of Integrative Medicine, Dalian Medical University, Dalian 116021, China.

3. Center for Medical Research and Innovation, Shanghai Pudong Hospital, Fudan University Pudong Medical Center, Shanghai 201399, China.

Abstract: Photothermal therapy (PTT) is an emerging local tumor ablation technique with clinical translation potential. After the NIR-II laser irradiates the tumor, the photothermal agent Hu-Kaiwen ink (Ink) converts light energy into hyperthermia and maintains the temperature at 42-45°C, thus achieving a low-temperature photothermal therapy. Alkyl radicals can kill tumor cells by overcoming the hypoxic microenvironment of the tumor. The photothermal reaction can induce the conversion of alkyl radicals from 2,2′-azobis[2-(2-imidazolin-2-yl) propane] dihydrochloride (AIPH) and thus have a synergistic tumor inhibition effect. the DNA methyltransferase inhibitor decitabine (DCT) can induce pyroptosis and cause inflammation and immune response to achieve systemic immunity. In this way, a synergistic combination of photothermal, alkyl radicals and pyroptosis could be used to kill breast tumor cells. Sodium alginate (ALG) was used as a carrier to form a hydrogel structure, which can improve the stability and duration of action of the mixed drugs. The significant tumor growth inhibitory effect of composite hydrogels has been demonstrated in both in vitro and ex vivo studies.

Keywords: Alkyl radical; Pyroptosis; Low-temperature photothermal therapy; Hydrogel; Breast cancer

1. Introduction

In 2020, there was nearly 2.3 million new cases of breast cancer in women around the world, making it the leading cancer in the world in terms of new cases [1]. Currently, the most common clinical treatments for breast cancer are surgery, chemotherapy, targeted therapy, immunotherapy and endocrine therapy. For the past few years, combination therapies have more applications in cancer treatment.

Alkyl radicals have received much attention in anti-tumor because this approach can kill tumor cells in a hypoxic microenvironment within the tumor [2]. In this subject, 2,2′-azobis[2-(2-imidazolin-2-yl) propane] dihydrochloride (AIPH) was used as an alkyl radical donor, which is capable of generating alkyl radicals at high temperatures. Even under hypoxic conditions, alkyl radicals could be generated and induce apoptosis by increasing intracellular lipid peroxidation [3].

Photothermal therapy (PTT) was used as a synergistic treatment to induce the conversion of alkyl radicals within the tumor. A photothermal agent with high photothermal conversion efficiency was used in PTT to convert exogenous light energy into hyperthermia under near-infrared (NIR) laser irradiation, resulting in localized hyperthermia at the tumor site, which in turn kills tumor cells [4]. The subject used low-temperature photothermal therapy (<45°C) by NIR-II laser irradiation to produce hyperthermia that inhibited tumor growth while inducing rapid conversion of AIPH to generate cytotoxic alkyl radicals [5]. Hu-Kaiwen ink (Ink) with good photothermal conversion rate was adopted as a photothermal agent.

As AIPH and Ink are fluid and easily degradable when administered as a liquid, it is important to select a suitable biomaterial as a drug carrier to improve stability and prolong drug release [6]. Sodium alginate (ALG) is a commonly used hydrogel material because of its low toxicity, good biocompatibility and biodegradability [7]. Moreover, ALG has the ability to exchange ions with multivalent cations and forms hydrogels under mild physiological conditions [8]. In view of the good drug-carrying capacity and gel-forming properties, ALG was adopted to immobilize the drug mixture in the tumor for a long time.

Pyroptosis is a form of programmed cell death and the onset of pyroptosis releases contents with inflammatory characteristics. The Gasdermin family is the main executor of pyroptosis. One of the most recently discovered mechanisms of pyroptosis is that Caspase-3 is able to cleave the DMLD sequence in GSDME, thereby inducing pyroptosis [9]. In this subject, photothermal therapy and cytotoxic radicals were used to activate caspase-3 to cleave the sensitive sequence of GSDME and induce pyroptosis. Most tumor cells express much lower GSDME than normal cells due to in vivo Deafness Autosomal Dominant 5 (DFNA5) promoter methylation [10,11]. DNA methyltransferase (DNMT) inhibitors can deregulate DNA methylation modifications and restore normal expression of functional proteins. In this study, the DNMT inhibitor decitabine (DCT) was used to demethylate the promoter of the methylated DFNA5 gene and to increase the expression of GSDME in tumor. Caspase-3 were activated by photothermal treatment and alkyl radicals, which can cleave the sensitive sequence of GSDME and induce pyroptosis. Finally, pyroptosis could cause an inflammatory response and an immune response to achieve a systemic immune response that completely kills tumor cells and prevents metastasis and recurrence.

2. Materials and experimental

2.1 Animals

BALB/c mice (female, 6−8 weeks of age) were acquired from Chang Sheng Biotechnology Corporation (Liaoning, China). Animal experiments were performed in accordance with the Guidelines for Animal Experiments of Dalian Medical University.

2.2 Preparation and characterization of hydrogel

Free Ink solution and Ink+ ALG (ALG 5 mg/mL；Ink 0.2 mg/mL) were Separately injected into $CaCl_2$ (Aladdin, China) solution (1.8 mmol/L). Successive photographs were taken to determine the synthesis of the composite hydrogel.

The Ink (Hu-Kaiwen, China) and ALG mixture, AIPH (Aladdin, China) and ALG mixture and DCT (Aladdin, China) and ALG mixture were prepared separately. Each mixture was injected into $CaCl_2$ (1.8 mmol/L) solution and photographs of each group were taken at 0 h and 24 h. The UV absorption of the supernatant of each group was detected using UV-vis to determine drug release.

2.3 Photothermal effects

H_2O, ALG, AIPH, DCT, Ink, DCT+ AIPH+ Ink+ ALG solutions were separately irradiated with laser (1064 nm, 0.5 W/cm^2, 10 min) and the temperatures were recorded by infrared thermal imager (Filr, USA).

2.4 Generation of intracellular free radicals

Different compositions including AIPH (50 μg/mL), Ink (25 μg/mL), ALG (1 mg/mL), DCT (10 μg/mL) and were added to 4T1 cells, with or without 1064 nm laser (0.5 W/cm^2, 10 min). DCFH-DA (Sigma-Aldrich, USA) working solution and DAPI staining were added sequentially to each group of confocal culture dishes, respectively. Confocal microscopy was used for observation.

2.5 Morphology of pyroptosis

After administration of the drug as in the previous method, the cells were placed under an inverted fluorescent microscope (Olympus, Japan) and photographed in white light for cell morphology.

2.6 Release of lactate dehydrogenase (LDH)

After administration of the drug as in the previous method, the prescribed amount of LDH releaser and the assay working solution were added to the corresponding cell samples in turn according to the procedure of the LDH cytotoxicity assay kit (Beyotime, China). Incubate for the prescribed time and measure the absorbance at 490nm.

2.7 Release of intracellular Ca^{2+}

After administration of the drug as in the previous method, Fluo-3 AM Calcium fluorescent probe working solution and DAPI solution were added to each group of cells in turn. Confocal microscopy was used for observation.

2.8 Cytotoxicity in vitro

AIPH, Ink, DCT and AIPH+ Ink+ DCT+ ALG composite hydrogel (ALG 1 mg/mL, Ink 25 μg/mL, AIPH 20 μg/mL, DCT 10 μg/mL) were added to 4T1 cells, with or without 1064 nm laser (0.5 W/cm^2, 10 min). Cell viability was assessed using the Cell Counting Kit-8 (CCK-8, KeyGen, China) after 24 hours of incubation.

2.10 In vivo synergistic cancer therapy

Thirty female BALB/c mice were inoculated with 0.1 mL of 4T1 cell suspension (1×10^7 cells) on their breast pads and experiments were performed when tumors grew to 100 mm^3.

50μL of the corresponding reagent in each group were injected into the tumor. After different administration for each group of mice, weight and subcutaneous tumor size were measured every other day throughout the treatment. And the tumors in each group were removed after 15 days of treatment. Tumor volume and tumor growth inhibition rate (IR) were calculated using the following formulae.

$$V\ (mm^3) = 0.5\times W^2\times L$$

$$IR= (W_{blank}- W_{treat})/W_{blank}\times 100\%$$

2.11 Data analysis and statistics

Statistical differences between the two groups were assessed with the unpaired student t-test. Multiple group comparisons were performed by the Bonferroni test for two-way ANOVA. *$p< 0.05$ was considered statistically significant. All data are expressed as mean± standard deviation.

3. Results and discussion

3.1 Preparation and characterization of hydrogel

As illustrated in Fig. 1A, the free Ink instilled into the Ca^{2+} solution diffused rapidly, which couldn't achieve controlled release of the drug. When the composite hydrogels were injected into the Ca^{2+} solution, a black hydrogel was seen among the solution and no significant diffusion of the black Ink solution occurred. After 24 h, the form of hydrogel was intact and black ink was released, proving that the composite hydrogels could play a good role in controlled drug release. In addition, according to our previous experiments, ALG concentration of 5mg/mL resulted in a better state of gel formation [12].

Fig. 1.

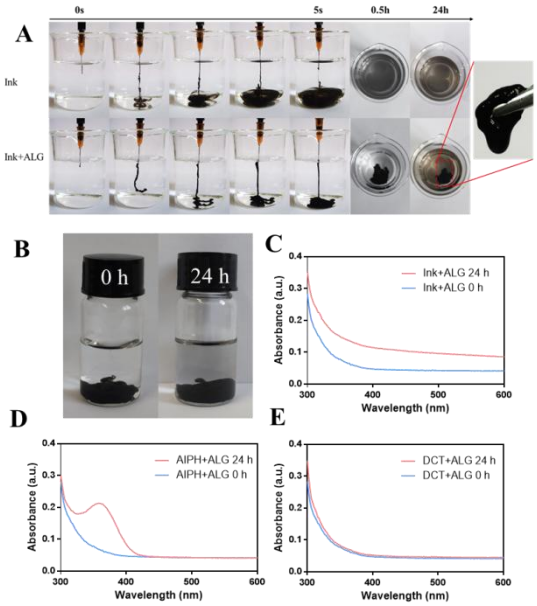

Subsequently, the release behaviors of the components in the composite hydrogels were investigated. After 24 h of constant temperature shaking experiment, the solution of the composite hydrogel changed from colorless to black, demonstrating the release of the drug from the ALG and Ca^{2+} cross-linkage (Fig. 1B). To further investigate the drug release capacity, the UV-vis spectra of the components in the composite hydrogels were analyzed (Fig. 1C-E). Compared to the absence of UV-visible absorption at 0 h, the supernatants of all groups exhibited varying degrees of absorbance after 24 h, indicating the release of Ink, AIPH and DCT from the hydrogels.

3.2 Photothermal effects of composite hydrogel

It was found that the H2O, ALG, AIPH and DCT in the composite hydrogels did not change in temperature after 10 min of laser irradiation by a 1064 nm laser, proving that they had no photothermal properties. Only when Ink was present in the composite hydrogels, its temperature rose gradually with time after laser irradiation, proving that only Ink had photothermal conversion properties in the composite hydrogels (Fig. 2A-B). What's more, the concentration of 25 μg/mL of Ink was selected for the subsequent study according to our previous experiments [12].

Fig. 2.

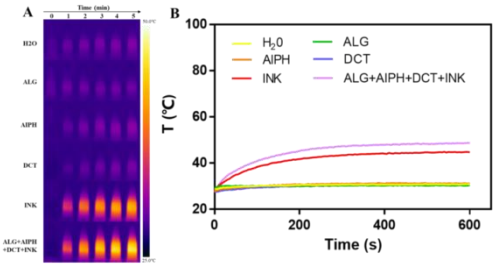

3.3 Detection of intracellular alkyl radicals

As indicated in Fig. 3, strong green fluorescence was visible under confocal microscopy in the DCT+ AIPH+ Ink+ ALG+ laser, DCT+ AIPH+ Ink+ laser and AIPH+ Ink+ ALG+ laser groups, while the green fluorescence signal was weak in the other groups. The experimental groups that included both AIPH and Ink and used laser irradiation could generate a

variety of free radicals, demonstrating that the heat generated by photothermal treatment could cause rapid conversion of cytotoxic alkyl radicals from AIPH. DCFH-DA was used to detect the alkyl radicals in 4T1 cells, as it can be oxidized by intracellular free radicals to produce green fluorescence [13].

Fig. 3.

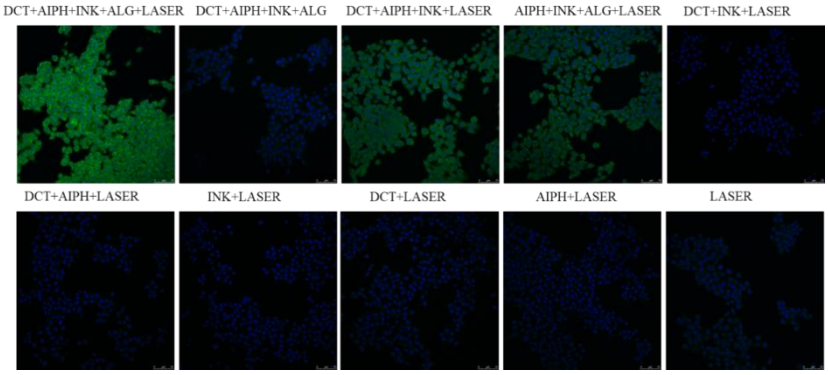

3.4 Pyroptosis caused by composite hydrogels

As shown in Fig. 4A, cells in the DCT+ AIPH+ Ink +ALG+ Laser group, DCT+ AIPH+ Ink+ Laser group and DCT+ Ink+ Laser group showed typical morphological changes of pyroptosis: cells bulged and produced bubbles. Some cells in the AIPH+ Ink+ Laser group and Ink+ Laser group showed apoptotic morphology such as smaller cell size, deformation and crumpling. The cell morphology of the other groups did not change significantly. It has been reported that the Gasdermin-N structural domain binded to membrane phospholipids and perforated the cell membrane after pyroptosis occurs, disrupting the osmotic potential and leading to cell swelling and the production of large bubbles [14]. In addition, the apoptotic morphology of the cells appeared in AIPH+ Ink+ Laser group and Ink+ Laser group in the experiments presumably related to apoptosis caused by photothermal toxicity and the release of cytotoxic alkyl radicals from AIPH during the photothermal transition.

Loss of cell membrane integrity results in the release of cell contents into the culture medium, including LDH in the cytoplasm [15]. So LDH release is seen as an important indicator of the integrity of the cell membrane. As shown in Fig. 4B, the LDH release rates of DCT+ AIPH+ Ink+ ALG+ Laser group and DCT+ AIPH+ Ink+ Laser group were 30.31% and 32.74% respectively, which were significantly different from the 2.62% in the PBS control group. The high release rate of LDH demonstrated that the integrity of the cell membrane was disrupted by the administration of these two groups.

High levels of Ca^{2+} are not detected when the cells are intact. In contrast, pyroptosis punctures the cell membrane, which causes high levels of Ca^{2+} to flow outside the cell. As shown in Fig. 4C, a large amount of green fluorescence appeared around the cells in the DCT+ AIPH+ Ink+ ALG+ Laser group and the DCT+ AIPH+ Ink+ Laser group, demonstrating that there was a large Ca^{2+} efflux and the integrity of the cell membrane was disrupted.

In summary, the occurrence of pyroptosis after DCT+ AIPH+ Ink+ ALG+ Laser composite hydrogel administration could be inferred from the typical morphology of pyroptosis and the disruption of cell integrity.

Fig. 4.

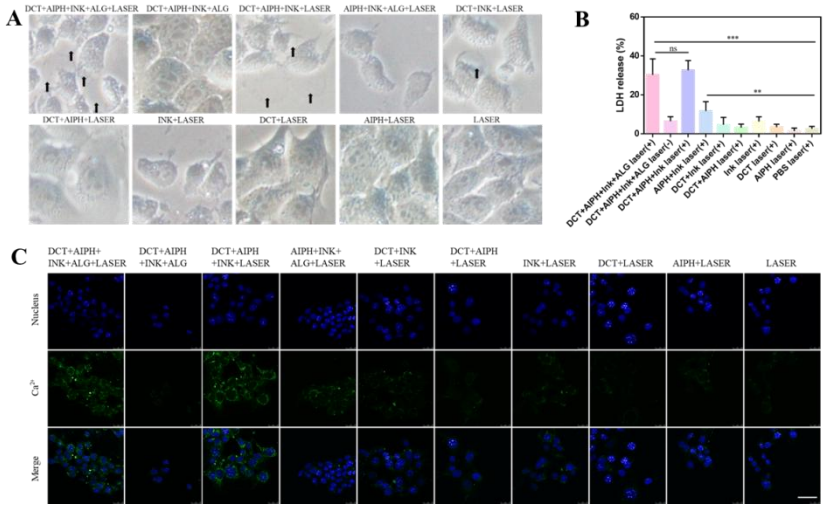

3.5 In vitro cytotoxicity of composite hydrogels

As illustrated in Fig. 5A-B: After incubation with different concentrations of DCT (0-40 μg/mL) and AIPH (0-50 μg/mL) solutions, cell viability values were high with or without laser irradiation, indicating that AIPH and DCT had no photothermal properties and had no cytotoxic to 4T1 breast cancer cells within the concentration range tested. As shown in Fig. 5C, cell viability values were high in the group without laser irradiation after incubation with different concentrations of Ink (0-100 μg/mL) solution. In the laser-irradiated group, the cell viability values were high in the concentration range of 0-50 μg/mL. but when 100 μg/mL of Ink was incubated with laser irradiation, the cell viability values decreased significantly and the cell survival rate was only 20.07%.

Two groups of composite hydrogels with different concentrations of AIPH were used in parallel to incubate 4T1 cells for 24 h. As shown in Fig. 5D, the group without laser irradiation showed good cell activity. Only when the AIPH concentration was increased to 100 μg/mL, the cell viability values decreased slightly. However, in the laser irradiated group, the cell viability decreased significantly with the increase of AIPH concentration. The cell viability value decreased sharply to 15.28% when the AIPH concentration was increased to 100 μg/mL. As a result, it could be proved that the synergistic administration of photothermal, alkyl radical and pyroptosis remarkably inhibited the growth of 4T1 breast cancer cells.

Fig. 5.

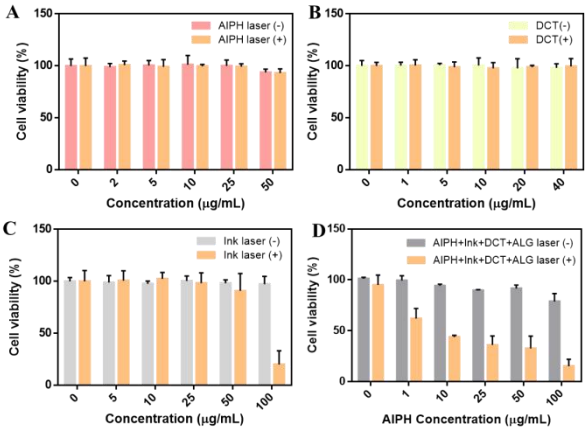

3.6 Antitumor effect and biocompatibility of composite hydrogels

The experimental protocol was shown in Fig. 6A. Fig. 6B showed the representative in situ tumor photographs peeled on day 15 of treatment, which demonstrated that DCT+ AIPH+ Ink+ ALG+ Laser composite hydrogel had the most significant tumor suppression effect. Fig. 6C showed the change curves of tumor growth volume in 4T1 tumor-bearing mice after administration of different treatment groups. After 15 days of treatment, the DCT+ AIPH+ Ink+ ALG+ Laser composite hydrogel group had the slowest tumor volume growth and the smallest tumor volume. Meanwhile, Fig. 6D showed the tumor inhibition rate of mice after administration of different treatment groups. The DCT+ AIPH+ Ink+ ALG+ Laser composite hydrogel administration group had the highest tumor inhibition rate of 85.81%. However, the tumor inhibition rate of the DCT+ AIPH+ Ink+ Laser administration group was only 47.56%, indicating that the loss of the hydrogel structure caused rapid metabolism of the drug in vivo, making it difficult to achieve a good therapeutic effect. Notably, none of the groups of mice showed significant fluctuations in body weight (Fig. 6E), indicating high biological safety of composite hydrogels. In summary, we concluded that the DCT+ AIPH+ Ink+ ALG+ Laser composite hydrogel had a highly synergistic tumor suppression effect.

Fig. 6

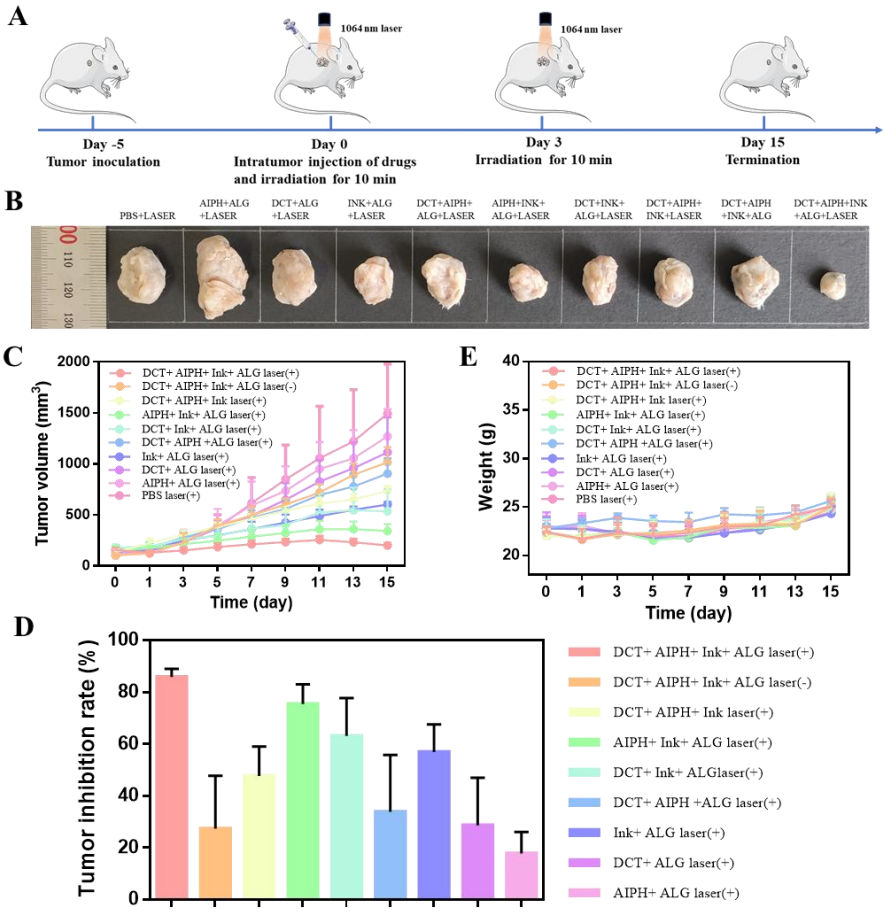

4. Conclusion

A composite hydrogel with sodium alginate as carrier was successfully established in this project. The treatment of breast tumors was achieved in a synergistic way with photothermal therapy, alkyl radicals and pyroptosis in combination.

The significant tumor growth inhibitory effect of DCT+ALG+ Ink+ ALG+ Laser composite hydrogel has been demonstrated in both in vitro and ex vivo studies. Additionally, this composite hydrogel strategy had a highly effective tumor suppression effect and high biological safety, which would pave a new route for the controllable, accurate, and coordinated tumor treatments.

5. Acknowledgements

This work was supported by the Key R&D Projects of Liaoning Province (2020JH2/10300046).

References

[1] Sung H, Ferlay J, Siegel RL, Laversanne M, Soerjomataram I, Jemal A, Bray F. Global Cancer Statistics 2020: GLOBOCAN Estimates of Incidence and Mortality Worldwide for 36 Cancers in 185 Countries[J]. CA Cancer J Clin, 2021, 71(3).

[2] Xiang H, Lin H, Yu L, Chen Y. Hypoxia-Irrelevant Photonic Thermodynamic Cancer Nanomedicine[J]. ACS Nano, 2019, 13(2).

[3] Chen ZH, Saito Y, Yoshida Y, Niki E. Effect of oxygen concentration on free radical-induced cytotoxicity[J]. Biosci Biotechnol Biochem, 2008, 72(6).

[4] Jaque D, Martinez Maestro L, Del Rosal B, Haro-Gonzalez P, Benayas A, Plaza J L, Martin Rodriguez E, Garcia Sole J. Nanoparticles for photothermal therapies[J]. Nanoscale, 2014, 6(16).

[5] Liao W, Ning Z, Chen L, Wei Q, Yuan E, Yang J, Ren J. Intracellular antioxidant detoxifying effects of diosmetin on 2,2-azobis(2-amidinopropane) dihydrochloride (AAPH)-induced oxidative stress through inhibition of reactive oxygen species generation[J]. J Agric Food Chem, 2014, 62(34).

[6] Cai Y, Si W, Huang W, Chen P, Shao J, Dong X. Organic Dye Based Nanoparticles for Cancer Phototheranostics[J]. Small, 2018, 14(25).

[7] Maity C, Das N. Alginate-Based Smart Materials and Their Application: Recent Advances and Perspectives[J]. Top Curr Chem (Cham), 2021, 380(1).

[8] Pan H, Zhang C, Wang T, Chen J, Sun S K. In Situ Fabrication of Intelligent Photothermal Indocyanine Green-Alginate Hydrogel for Localized Tumor Ablation[J]. ACS Appl Mater Interfaces, 2019, 11(3).

[9] Wang Y, Gao W, Shi X, Ding J, Liu W, He H, Wang K, Shao F. Chemotherapy drugs induce pyroptosis through caspase-3 cleavage of a gasdermin[J]. Nature, 2017, 547(7661).

[10] Akino K, Toyota M, Suzuki H, Imai T, Maruyama R, Kusano M, Nishikawa N, Watanabe Y, Sasaki Y, Abe T, Yamamoto E, Tarasawa I, Sonoda T, Mori M, Imai K, Shinomura Y, Tokino T. Identification of DFNA5 as a target of epigenetic inactivation in gastric cancer[J]. Cancer Sci, 2007, 98(1).

[11] Kim MS, Chang X, Yamashita K, Nagpal JK, Baek JH, Wu G, Trink B, Ratovitski EA, Mori M, Sidransky D. Aberrant promoter methylation and tumor suppressive activity of the DFNA5 gene in colorectal carcinoma[J]. Oncogene, 2008, 27(25).

[12] Ouyang B, Liu F, Ruan S, Liu Y, Guo H, Cai Z, Yu X, Pang Z, Shen S. Localized Free Radicals Burst Triggered by NIR-II Light for Augmented Low-Temperature Photothermal Therapy[J]. ACS Appl Mater Interfaces, 2019, 11(42).

[13] Huang G, Qiu Y, Yang F, Xie J, Chen X, Wang L, Yang H. Magnetothermally Triggered Free-Radical Generation for Deep-Seated Tumor Treatment[J]. Nano Lett, 2021, 21(7).

[14] Wu D, Wang S, Yu G, Chen X. Cell Death Mediated by the Pyroptosis Pathway with the Aid of Nanotechnology: Prospects for Cancer Therapy[J]. Angew Chem Int Ed Engl, 2021, 60(15).

[15] Feng Y, Xiong Y, Qiao T, Li X, Jia L, Han Y. Lactate dehydrogenase A: A key player in carcinogenesis and

potential target in cancer therapy[J]. Cancer Med, 2018, 7(12).

Figure Legends

Fig. 1. Characterization of composite hydrogels. (A) Photographs of hydrogel formation at different time points after Ink and Ink+ ALG were injected into $CaCl_2$ solution respectively (ALG 5 mg/mL). (B) Changes in the appearance of drug release from composite hydrogels in $CaCl_2$ solutions for 24 h. (C)-(E) UV-vis absorption spectra of Ink, AIPH and DCT in the supernatant of the composite hydrogel after 24 h in $CaCl_2$ solution.

Fig. 2. Photothermal properties of composite hydrogels. (A) Infrared thermograms of different components of the composite hydrogel under 1064 nm laser irradiation (0.5 W/cm^2, 10 min). (B) Photothermal curve corresponding to Fig. 2A.

Fig. 3. Confocal images of alkyl radical in 4T1 breast cancer cells after different dosing treatments, bar= 75 μm.

Fig. 4. Pyroptosis induced by composite hydrogel. (A) Morphology of cells after different treatments. (B) LDH release after different treatments. (C) Intracellular Ca^{2+} concentration after different treatments, bar= 50 μm. P values: * $p < 0.05$; ** $p < 0.01$; *** $p < 0.001$.

Fig. 5. In vitro cytotoxicity of composite hydrogels. Relative cell viabilities of 4T1 cells after 24 h incubation with or without laser irradiation for different concentrations of (A) AIPH, (B) DCT and (C)Ink, respectively. (D) Relative cell viabilities of 4T1 cells after 24 h incubation with or without laser irradiation in composite hydrogels at different AIPH concentrations and constant concentrations of other components.

Fig. 6. In vivo synergistic therapeutic effect of composite hydrogels. (A) Schematic diagram of the therapeutic experiment. (B) Representative photographs of the in situ tumor removed after day 15 of treatment. (C) Tumor growth curves in 4T1 tumor-bearing mice after various treatment, n= 5. (D) Body-weight changes during 15 days, n= 5. (E) Tumor growth inhibition after various treatment, n= 5.